IRBM 46 (2025) 100918

Contents lists available at ScienceDirect

IRBM

journal homepage: www.elsevier.com/locate/irbm

Elsevier Masson France

EM|consulte

www.em-consulte.com

Brief Report

Assessment of Stress Distributions in a Skeletal Muscle Affected by Post-Stroke Spastic Myopathy

Kalthoum Belghith, Ali Aghaei, Wael Maktouf, Mustapha Zidi *

Bioengineering, Tissues and Neuroplasticity, UR 7377, Université Paris-Est Créteil, Faculté de Santé/EPISEN, 8 rue du Général Sarrail, 94010 Créteil, France

HIGHLIGHTS

- Shear modulus measured in the medial gastrocnemius of post-stroke patients.
- Finite element analysis estimated stress distributions under uniform stretch.
- Post-stroke muscles exhibited higher stress concentrations.

GRAPHICAL ABSTRACT

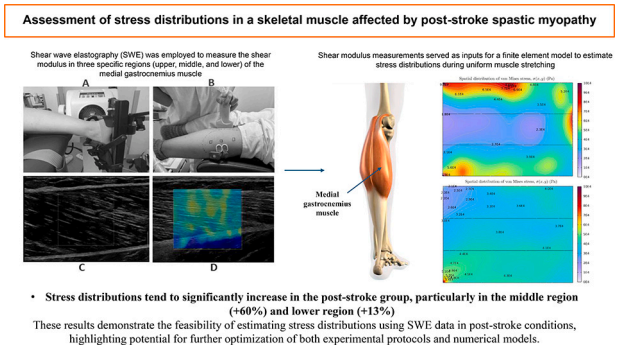

ARTICLE INFO

Article history:
Received 13 February 2025
Received in revised form 13 October 2025
Accepted 27 October 2025
Available online 29 October 2025

Keywords:
Skeletal muscle
Post-stroke spasticity
Shear wave elastography
Finite element method, stress distributions

ABSTRACT

This study aims to evaluate stress distributions in the medial gastrocnemius muscle (GM) of patients with spastic myopathy after stroke. Shear wave elastography was employed to measure the shear modulus in three specific regions (upper, middle, and lower) of the muscle in six participants (three healthy and three post-stroke). Shear modulus measurements served as inputs for a finite element model to estimate stress distributions during uniform muscle stretching. The skeletal muscle was modeled as a hyperelastic, incompressible, and inhomogeneous material. The results showed that the stress distribution tends to increase in the post-stroke group, particularly in the middle (+60%) and lower regions (+13%). These results demonstrate the feasibility of estimating stress distributions using SWE data in post-stroke conditions, highlighting potential for further optimization of both experimental protocols and numerical models. These advancements could ultimately provide valuable insights into the clinical challenges associated with understanding spastic myopathy pathologies.

1. Introduction

Spastic myopathy following a stroke is a debilitating condition characterized by persistent muscle stiffness and involuntary contractions [14,19]. This condition significantly impacts skeletal muscles, leading to alterations in muscle structure and function [3]. The combination of spasticity and muscle weakness can contribute to reduced mobility and decreased quality of life for affected individuals [25]. Understanding the consequences of spastic myopathy on skeletal muscle mechanics properties is crucial for improving rehabilitation and treatment strategies.

For that, recent studies have increasingly employed shear wave elastography (SWE) to investigate muscle stiffness [24] with experimental technics. SWE functions by transmitting an acoustic pressure wave into biological tissues, resulting in the generation of slower lateral oscillations known as shear waves [31]. By measur-

* Corresponding author.
E-mail addresses: kalthoum.belghith@u-pec.fr (K. Belghith), ali.aghaei@u-pec.fr (A. Aghaei), wael.maktouf@u-pec.fr (W. Maktouf), zidi@u-pec.fr (M. Zidi).

https://doi.org/10.1016/j.irbm.2025.100918

ing the velocity of these waves, SWE facilitates the determination of shear modulus, allowing for a localized, non-invasive assessment of muscle stiffness across different joint positions and muscle conditions. Several studies have consistently demonstrated heightened stiffness in paretic muscles of stroke survivors. For example, Jakubowski et al. [18] reported that the shear modulus of the medial gastrocnemius increased significantly as the ankle joint transitioned from plantarflexion to dorsiflexion, with greater stiffness observed in the paretic limb compared to the non-paretic side.

Additionally, numerical modeling serves as a valuable tool for characterizing muscle as a complex biological material with properties such as elasticity, viscosity, and plasticity [23]. Constitutive models, based on the principles of material mechanics, are developed to simulate the muscle's response to various mechanical loads. These models often utilize medical imaging data, such as MRI [10], to create realistic simulations of muscle behavior. For instance, Grasa et al. [16] used finite element modeling to develop a 3D model of the rat tibialis anterior (TA) muscle, accurately simulating both passive (stretching) and active (contraction) states. In their model, a constitutive relation based on a strain energy function (SEF) was implemented, capturing the contributions of both active and passive responses by fitting experimental data. The model incorporated the tissue's initial deformations and employed a quasi-incompressible formulation of a transversely isotropic material. MRI images were used to reconstruct the external geometry of the TA muscle, including these initial deformations [16]. The numerical results demonstrated excellent consistency with experimental data, particularly in comparing force-extension curves for both passive and active tests. This confirms the ability of the model to predict muscle behavior under various loading conditions.

In their study, Xu et al. [30] addressed this limitation by proposing a novel SWE method to infer the active constitutive parameters of skeletal muscles in vivo. To achieve this, they examined the propagation of shear waves through skeletal muscles, which are described by a constitutive model that incorporates an active muscle behavior parameter. An analytical solution was derived to relate shear wave velocities to the passive and active material parameters of muscles [30]. Based on this solution, an inverse approach was developed to estimate these parameters. The results revealed that the active material parameters of skeletal muscles vary according to factors such as warm-up, fatigue, and rest, providing new insights into the dynamic mechanical properties of muscles.

While this study focused on healthy muscles, it would be interesting to extend this approach to pathological muscles, particularly those affected by spastic myopathy. This could provide a better understanding of the microstructural degradations associated with this condition [7]. Moreover, investigating the alterations in muscle stiffness and active behavior in spastic myopathy could offer valuable insights into the extent of muscle damage and the mechanisms underlying impaired muscle function. Such research could not only enhance our understanding of the disease progression, but also provide critical information for developing targeted rehabilitation strategies aimed at restoring muscle function and mitigating the impacts of spasticity [5].

Note that few of these previous studies have investigated the stress distributions in skeletal muscle with spastic myopathy after stroke. In the case of spastic myopathy, skeletal muscle undergoes structural changes (fibrosis, replacement by adipose tissue, etc.) and functional changes (hypertonia, involuntary contractions) [2,20,26]. As spastic myopathy progresses, stresses within the muscle change, leading to mechanical alterations that can disrupt muscle function. Indeed, excessive stress in a spastic muscle can lead to joint strains, stress fractures, or loss of mobility [14]. Therefore, estimating these stresses could provide a better understanding of the underlying pathological mechanisms. Moreover, such estimations would allow for the monitoring of alterations in muscle properties, including increased fiber stiffness and reduced elasticity of the surrounding connective tissue. This, in turn, could guide the optimization of clinical interventions and the design of targeted exercise programs. This study aims to propose a method for estimating stress distributions in skeletal muscle affected by post-stroke spastic myopathy. To achieve this, a numerical finite element approach utilizing shear modulus measurements obtained through SWE is proposed. The analysis of stress distributions allows for the comparison between healthy muscles and those of patients with spastic myopathy after stroke.

Table 1
Subject characteristics.

Characteristics of participants	CNT (n=3)	SSG (n=3)	*p*
Sex (male: female)	1: 2	1: 3	–
Age (y)	39.3 ± 7.33	56.2 ± 6.43	NS
Height (m)	1.66 ± 0.06	1.70 ± 0.19	–
Weight (kg)	67.6 ± 12.01	71.32 ± 12.81	–
BMI* ($kg.m^{-2}$)	23.14 ± 3.68	24.16 ± 2.96	–
Time post-stroke (months)	NA	5.56 ± 1.04	NS
Affected side (R: L)	NA	2: 4	–

2. Material and methods

2.1. Subjects

Six participants were recruited from the neurological rehabilitation department of a rehabilitation clinic and divided into two groups (Table 1). The control group (CNT) consisted of 3 healthy participants with no history of neurological or muscular disorders. The stroke survivor group (SSG) consisted of 3 Stroke survivors with spastic hemiparesis. The inclusion criteria for the SSG were adults 20 to 75 years of age with chronic hemiparesis (>6 months). Participants were informed of the nature of the study before providing written informed consent. The study received Institutional Ethics Committee approval (CPP 2022–038 = 000117). The procedures were conducted according to the principles expressed in the Declaration of Helsinki.

2.2. Materials

An Aixplorer® ultrasound elastography (Supersonic Imagine, version 6.1, Aix-en-Provence, France) was utilized in Shear Wave mode (musculoskeletal preset, penetration mode) to quantify muscle stiffness in the medial gastrocnemius muscle (GM). A linear ultrasound probe (4–15 MHz, SL15-4; SuperSonic Imagine, Aix-en-Provence, France) was positioned parallel to the muscle fibers, with acoustic gel applied as an interface between the probe and the skin. The generation and propagation of shear waves through adjacent tissues were tracked using a speckle-tracking algorithm. Displacement maps were then created to calculate the shear wave velocity (SWV, m/s) for each pixel of the map. The shear modulus (μ) was subsequently calculated using the formula: $\mu = \rho.SWV^2$ where ρ represents the muscle mass density, assumed to be 1000 kg/m^3.

Based on the anatomical landmarks [4], the medial region was identified for the GM using B-mode elastography. The probe location was marked on the skin using waterproof ink. The ultrasound images were then exported from the Aixplorer® software for further analysis and processing.

A Biodex System 4 Isokinetic Dynamometer (Medical Systems, Inc., Shirley, NY, USA) was utilized to assess passive mobilization. Participants were positioned in a prone posture with their knee fully extended and their hip in a neutral position (0°) (Fig. 1). The ankle joint was meticulously aligned with the dynamometer's axis

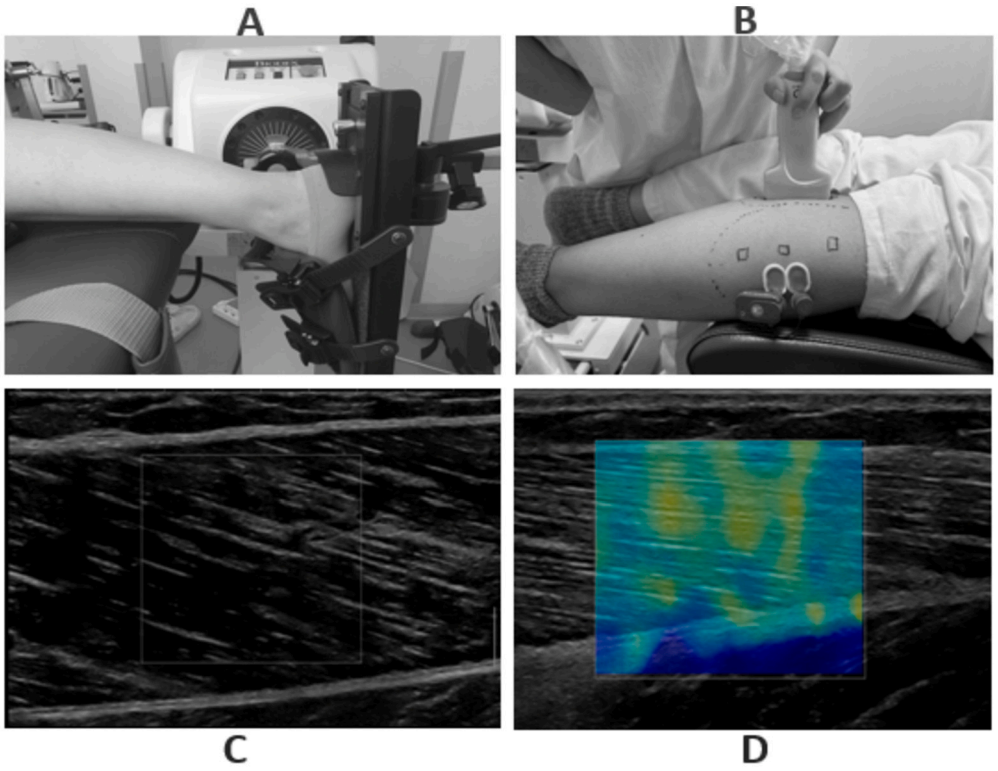

Fig. 1. Experimental set-up. A: Positioning of the ankle on the isokinetic system, B: Probe positioning, C: Identification of GM and GL muscles, D: Elastography image acquisition.

of rotation and placed in a fully relaxed state, which was designated as the 0° reference position for the isokinetic system. Then, the ankle was passively mobilized from 0° to dorsiflexion at a controlled angular velocity of 2°/s.

2.3. Data processing

Data processing was carried out using Matlab software (Matlab R2024a, MathWorks, Natick, USA). Following the general methodology described previously, we extracted a series of images from the recorded video, with each image associated with a DICOM file. Subsequently, we selected a specific region of interest (ROI) within the muscle, ensuring it was identical for each analyzed image. This approach ensures consistency and accuracy in measurements throughout the image analysis.

To calculate the force exerted on the GM, data files were extracted from the isokinetic system. The force exerted on the GM, denoted as F_{GM}, is defined by:

$$F_{GM} = \frac{(F_1 - F_2).0.61}{Cos(\theta_{pen})}, \tag{1}$$

where F_1 is the total force of the plantar flexors (PF) with the knee extended, F_2 is the total force of the PF with the knee flexed and θ is the pennation angle [32].

It should be noted that the proportion of the force specifically attributed to the medial gastrocnemius (as a subcomponent of the gastrocnemius) is 0.61 [13]. Additionally, for numerical simulations, F_{GM} was normalized by $F_{\mathrm{GM}}^{\max}$, to obtain $F_{GM} = [0, 1]$.

2.4. Finite element method (FEM)

The numerical study was performed using the finite element software COMSOL Multiphysics® 6.2. The data obtained via SWE were used to define the constitutive parameters of the skeletal muscle tissue. The 2D region of interest was meshed with first-order quadrilateral finite elements, with one side fixed (clamped) and the opposite side subjected to a tensile force (Fig. 2).

Additionally, it was assumed that skeletal muscle tissue behaves as a hyperelastic, isotropic, incompressible, and inhomogeneous material, described by the quasi-incompressible Neo-Hookean strain energy density function [1,33], which is expressed as:

$$W = \frac{\mu(x, y)}{2}(I_1 - 3) + \frac{k}{2}(J - 1)^2, \tag{2}$$

where $\mu\ (x, y)$, k and I_1 respectively represent the spatial shear modulus in the interest zone, the fixed volumetric parameter, and the first principal invariant of deformation [12].

Thus, only one material parameter is needed for the chosen hyperelastic law. The numerical simulations thus provided an estimate of the von-Mises stress distributions [12] in the three regions of the model (upper, middle, and lower zones).

It is important to note that von-Mises stresses serve as a criterion for assessing the risk of structural damage in skeletal muscle tissue. They can be utilized to model regions susceptible to mechanical overload or microtrauma during stretching, both in healthy and pathological muscle conditions.

3. Results

The von Mises stress distributions in the GM highlight key differences between healthy and stroke-affected muscles. In the healthy subject, the stress pattern appears relatively inhomogeneous, with higher concentrations in the upper and lower regions, while the middle region shows a more uniform and consistent distribution. This reflects a balanced mechanical behavior across the muscle (Fig. 3).

In contrast, the stroke survivor presents a more heterogeneous stress distribution, with a notably greater concentration in the

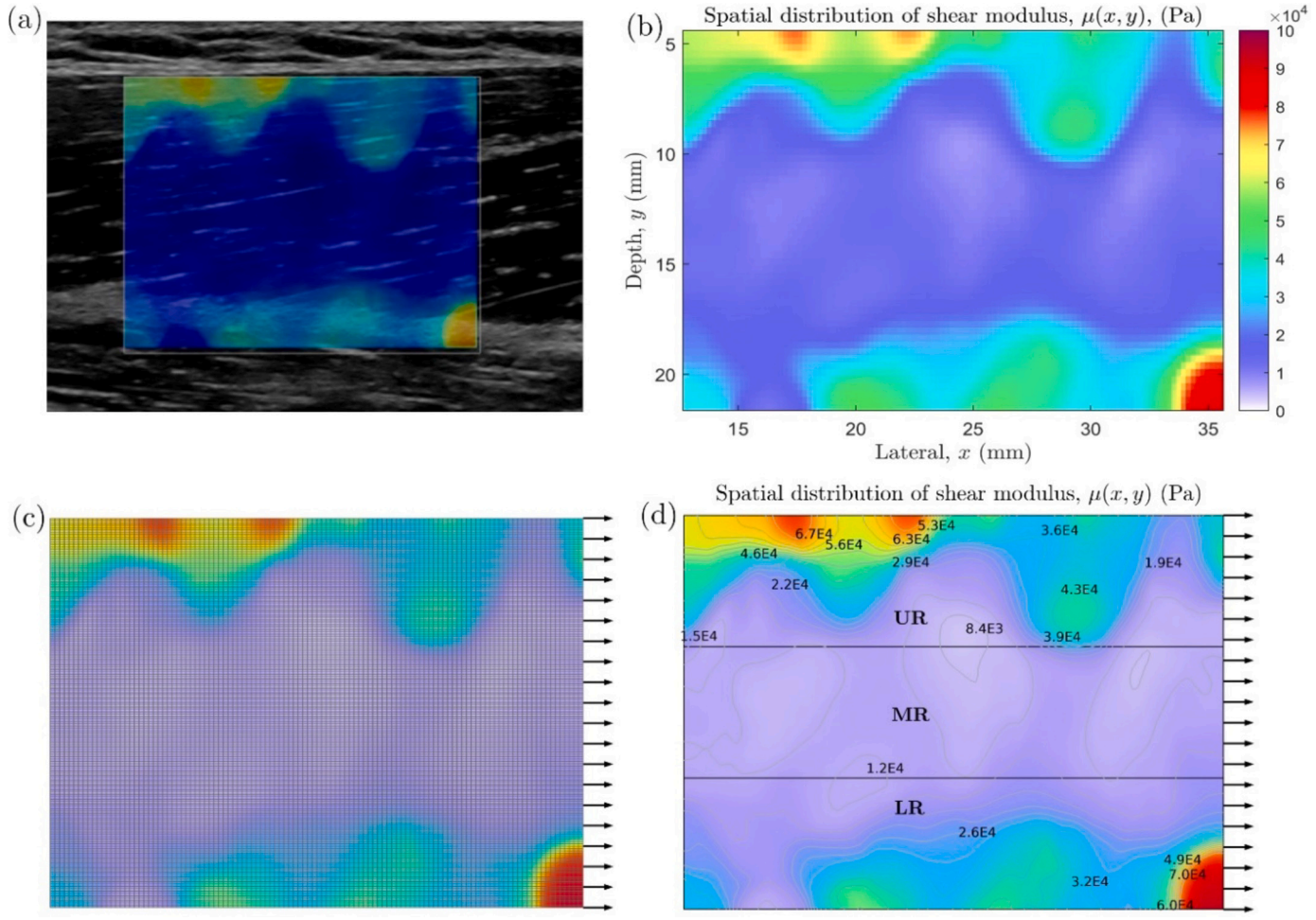

Fig. 2. Illustrative Example of Steps of Finite Element Numerical Simulation for Estimating Stress Distributions (in Pa) Using Shear Wave Elastography (SWE) Data (shear modulus in Pa). (a) Region of interest and mapping of experimental shear modulus values measured by SWE. (b) Shear modulus map processed using MATLAB software. (c) Meshing of the region of interest with boundary conditions and an applied force using COMSOL Multiphysics software. (d) Region of interest divided into three areas: upper (UR), middle (MR), and lower (LR) regions.

lower region. This change suggests disrupted internal muscle organization and altered mechanical response following stroke (Fig. 4).

The stress–stretch relationships further illustrate these differences. In healthy individuals, the von Mises stress (σ) increases non-linearly with stretch (λ), and the responses across the different muscle regions remain similar at lower stretch values. However, at higher stretch, differences become more pronounced, particularly in the upper and lower regions, where stiffness increases more rapidly, indicating preserved mechanical adaptability and tolerance (Fig. 5).

For stroke-affected muscles, the stress–stretch curves are more irregular between regions, with steeper slopes and less uniform behavior. The upper region reaches its maximal stress at a lower stretch ($\lambda \approx 1.3$) compared to other regions. This suggests increased rigidity, reduced elongation, and impaired structural integrity likely due to pathological changes such as fibrosis and fiber disorganization (Fig. 6). Note that pathological muscle stress distribution is often different because of structural alterations (fibrosis, fiber disorganization). Findings suggest that stroke-induced muscle alterations result in limited stretch capacity and greater resistance to stretch.

4. Discussion

This study aims to evaluate the mechanical stress distributions within the GM muscle in post-stroke survivors with spastic myopathy, compared to healthy individuals. These first results obtained through a finite element modeling (FEM) and the analysis of von-Mises stress-stretch relationships provide valuable insights into the mechanical alterations induced by post-stroke spastic myopathy.

4.1. Mechanical stress distributions

Von Mises stress maps reveal notable differences between healthy subjects and post-stroke survivors. In healthy subjects, the stress distribution appears relatively homogeneous, with higher concentrations in the proximal and distal regions of the GM. This is likely due to the convergence of aponeuroses in these areas. This uniform distribution suggests that a healthy muscle can effectively distribute mechanical loads during passive stretching, as seen in the stress mapping. In post-stroke survivors, the stress distribution is significantly more heterogeneous, with a marked concentration in the upper region of the muscle as elongation increases. This heterogeneity can be explained by factors specific to spastic myopathy. Altered mechanical properties of the paretic muscle due to increased collagen accumulation in key structures regulating muscle elasticity [8]. These structures include the perimysium (enveloping muscle bundles), myofibrils (responsible for muscle contraction), and titin (a giant protein crucial for muscle fiber integrity and passive stiffness) [15,17]. Also, the elevated col-

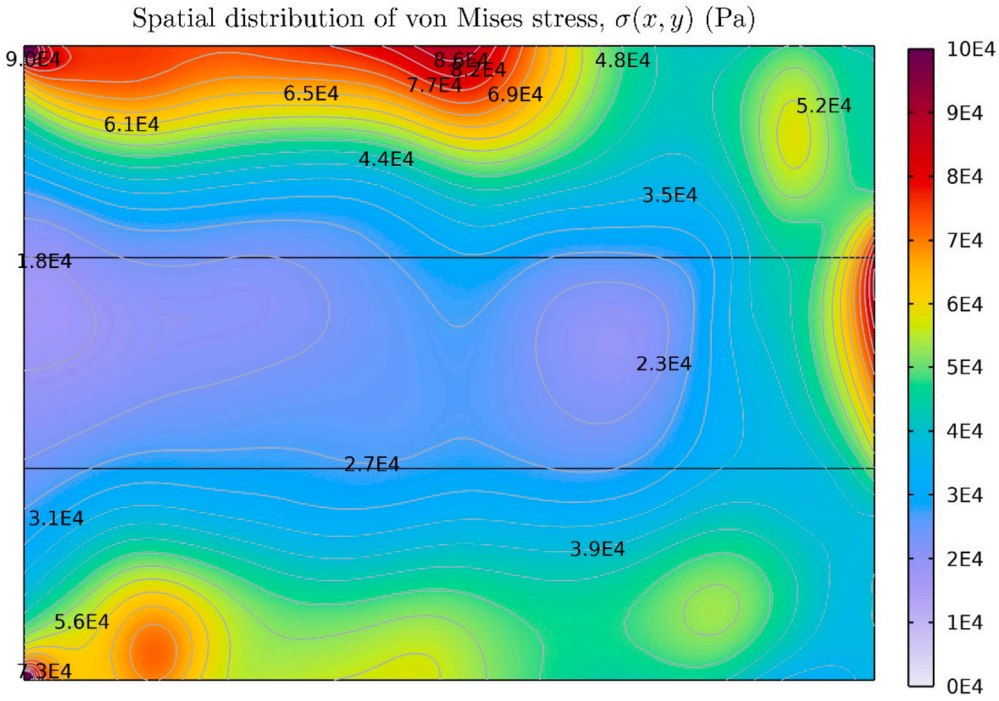

Fig. 3. Illustrative Example of Quantitative Mapping of Von Mises Stress Distributions (in Pa) Obtained by FEM for a Healthy Subject with $F_{GM} = 0.5$. This figure illustrates the stress distribution in the medial gastrocnemius across the three regions (upper, middle, and lower).

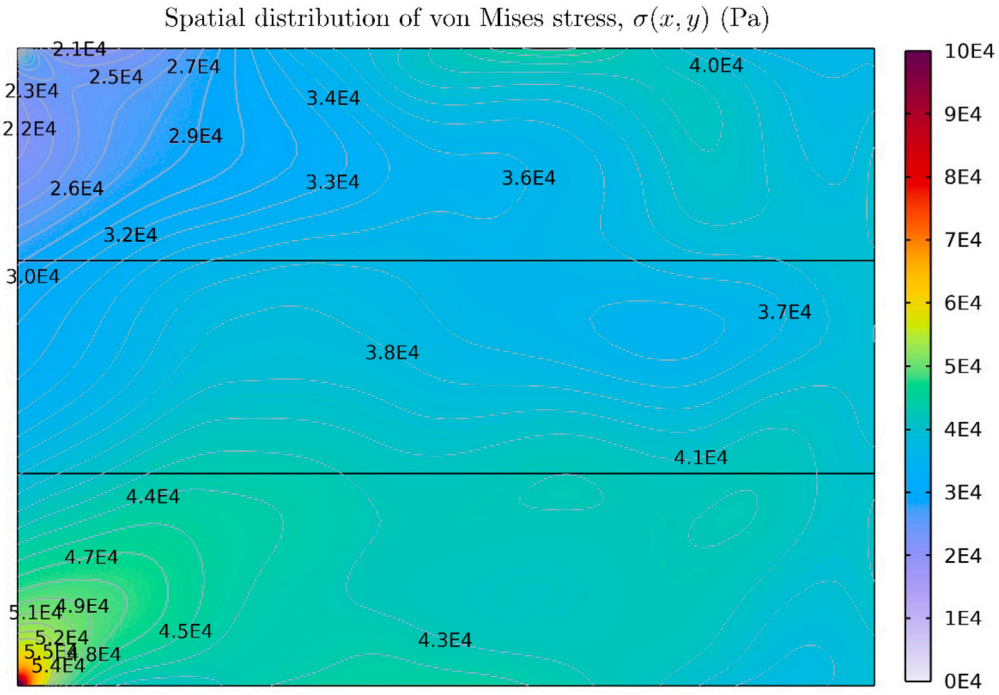

Fig. 4. Illustrative Example of Quantitative Mapping of Von Mises Stress Distributions (in Pa) Obtained by FEM for a Stroke Subject with $F_{GM} = 0.5$. This figure illustrates the stress distribution in the medial gastrocnemius across the three regions (upper, middle, and lower).

lagen content in these components can lead to increased muscle stiffening, reducing their ability to deform uniformly under stress [8,19].

Spastic myopathy may also alter the muscle's mechanical properties, leading to uneven stress distribution during stretching. Changes in innervation and muscle activation post-stroke might further contribute to the muscle's non-uniform mechanical response [21,27].

4.2. Force elongation relationship

The analysis of force-elongation relationships (Figs. 4 and 5) reveals important differences between healthy subjects and post-stroke survivors. In healthy subjects, the force-elongation curves for different muscle regions are quite similar, especially at higher stretch levels ($\lambda \geq 1.6$). This uniformity reflects a consistent and balanced mechanical response of the healthy muscle to passive

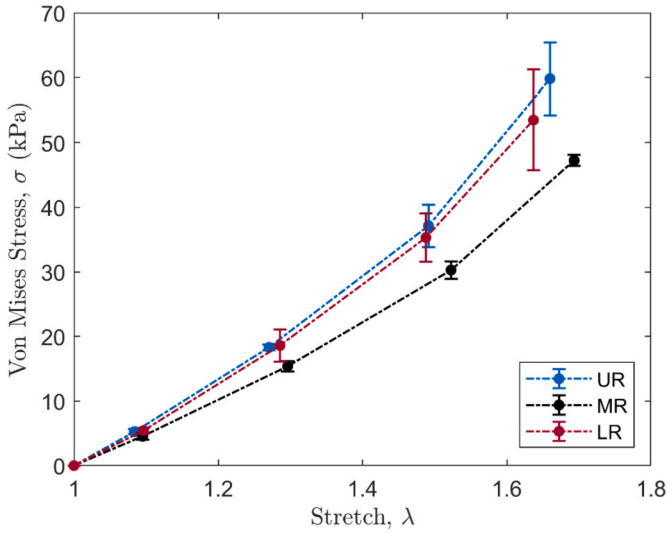

Fig. 5. Von-Mises stress -Stretch Relationship Across Muscle Regions in Healthy Subjects.

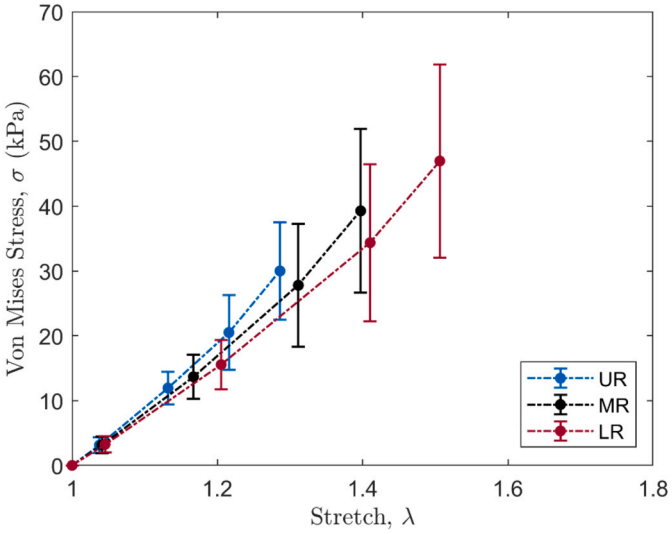

Fig. 6. Von-Mises Stress-Stretch Relationship Across Muscle Regions in Stroke Subjects.

stretching [11]. Force-elongation curves exhibit significant variability across muscle sub-regions, with steeper slopes indicating increased rigidity.

Notably, the lower sub-region of the GM reaches its maximum force at a lower stretch level ($\lambda \approx 1.6$) compared to the upper and middle sub-regions. This suggests increased stiffness or altered mechanical properties in the lower part of the muscle in patients with spastic myopathy. Gao et al. [13] investigated the effect of spastic paresis on GM mechanical properties and architecture, finding that during passive ankle mobilization, joint stiffness was significantly higher in post-stroke patients. This increased stiffness was associated with a notable reduction in fascicle length, aligning with our observations of reduced muscle elongation, particularly in the lower GM sub-region.

4.3. Clinical implications

Several clinical and physiological implications arise from these numerical findings. The reduced extensibility observed in post-stroke subjects, particularly in the lower GM region, suggests a loss of muscle flexibility, which could contribute to functional limitations, especially in walking and balance [13]. The reduction in fascicle length indicates significant structural changes that may explain the altered mechanical response of the muscle. These structural and functional modifications highlight the need for targeted therapeutic interventions aimed at improving muscle extensibility and motor function in post-stroke patients. Additionally, localized stress concentrations in certain regions of the muscle may increase the risk of injury during stretching or physical activity, emphasizing the need for tailored rehabilitation approaches. The regional differences in mechanical properties suggest that interventions could benefit from a localized approach, targeting areas with the greatest changes in stress distribution. These findings also underscore the importance of incorporating region-specific parameters into mechanical models of muscles affected by spastic myopathy, rather than treating the muscle as a homogeneous entity.

4.4. Limitations and perspectives

The primary limitations of this study include a small sample size, with only three participants per group, which limits the scope and generalizability of the findings. Although there are difficulties in recruiting people with spastic myopathy, future studies with larger sample sizes are needed to validate these observations and strengthen the conclusions. Additionally, this study's cross-sectional design provides only a snapshot of the mechanical properties of muscle tissue at a single point in time. A longitudinal approach, tracking participants over an extended period [9], would allow for the exploration of the evolution of mechanical alterations and their response to therapeutic interventions. On the other hand, we used a Neo-Hookean model to describe the passive mechanical behavior of the skeletal muscle tissue, which has the advantage of reducing the number of material parameters used. However, the anisotropic character of skeletal muscle tissue could be considered with another energy function [22,28,29]. This would require directional SWE measurements [6].

5. Conclusion

This study highlights significant alterations in muscle mechanical properties induced by post-stroke spastic myopathy. The observed heterogeneous stress distribution and regional variations in force-elongation relationships underscore the complexity of biomechanical changes associated with this condition. These findings suggest that the muscle's ability to respond uniformly to mechanical stress is compromised, particularly in certain regions of the muscle, which may contribute to the functional impairments commonly seen in post-stroke patients. The localized stiffness and altered stress distribution could lead to an increased risk of muscle injury and further contribute to difficulties in movement, such as impaired walking and balance.

CRediT authorship contribution statement

Kalthoum Belghith: Writing – original draft, Visualization, Validation, Methodology, Investigation, Funding acquisition, Formal analysis. **Ali Aghaei:** Writing – original draft, Validation, Software, Methodology, Investigation, Funding acquisition. **Wael Maktouf:** Writing – original draft, Visualization, Validation, Methodology, Funding acquisition, Formal analysis. **Mustapha Zidi:** Writing – original draft, Validation, Supervision, Methodology, Formal analysis, Conceptualization.

Author contributions

All authors attest that they meet the current International Committee of Medical Journal Editors (ICMJE) criteria for Authorship.

Informed consent and patient details

The authors declare that this report does not contain any personal information that could lead to the identification of the patient(s).

The authors declare that they obtained a written informed consent from the patients and/or volunteers included in the article. The authors also confirm that the personal details of the patients and/or volunteers have been removed.

Human and animal rights

The authors declare that the work described has been carried out in accordance with the Declaration of Helsinki of the World Medical Association revised in 2013 for experiments involving humans as well as in accordance with the EU Directive 2010/63/EU for animal experiments.

Funding

This work did not receive any grant from funding agencies in the public, commercial, or not-for-profit sectors.

Declaration of competing interest

The authors declare that they have no known competing financial or personal relationships that could be viewed as influencing the work reported in this paper.

Acknowledgements

This work was supported by University Paris-Est Créteil. The authors acknowledge the contribution of the medical staff and the managers of the “Clinique du Parc de Belleville” for their help in the recruitment and monitoring of patients and the organization of the conduct of the experimental protocol. This study was conducted with the support of Emeis group.

References

[1] Affagard J-S, Bensamoun SF, Feissel P. Development of an inverse approach for the characterization of in vivo mechanical properties of the lower limb muscles. J Biomech Eng 2014;136(11):111012.
[2] Baude M, Nielsen JB, Gracies J-M. The neurophysiology of deforming spastic paresis: a revised taxonomy. Ann Phys Rehabil Med 2019;62(6):426–30.
[3] Beckwée D, Cuypers L, Lefeber N, De Keersmaecker E, Scheys E, Wout VAN, et al. Skeletal muscle changes in the first three months of stroke recovery: a systematic review. J Rehabil Med 2022;54.
[4] Belghith K, Zidi M, Fedele J-M, Bou-Serhal R, Maktouf W. Dataset of Inter and intramuscular variability of stiffness in paretic individuals during prone and standing positions. Data Brief 2024;110190.
[5] Belghith K, Zidi M, Fedele J-M, Serhal RB, Maktouf W. Spatial distribution of stiffness between and within muscles in paretic and healthy individuals during prone and standing positions. J Biomech 2023;161:111838.
[6] Bied M, Gennisson J-L. Acoustoelasticity in transversely isotropic soft tissues: quantification of muscle nonlinear elasticity. J Acoust Soc Am 2021;150(6):4489–500.
[7] Bovio N, Abd GM, Ku JC, Liu LC, Li Y. A review on the mechanisms of stroke-induced muscle atrophy; 2024.
[8] de Bruin M, Smeulders MJ, Kreulen M, Huijing PA, Jaspers RT. Intramuscular connective tissue differences in spastic and control muscle: a mechanical and histological study. PLoS ONE 2014;9(6):e101038.
[9] Dorňák T, Justanová M, Konvalinková R, Říha M, Mužík J, Hoskovcová M, et al. Prevalence and evolution of spasticity in patients suffering from first-ever stroke with carotid origin: a prospective, longitudinal study. Eur J Neurol 2019;26(6):880–6.
[10] Feng L, Duan Q, Lai R, Liu W, Song X, Lyu Y. Development of a three-dimensional muscle-driven lower limb model developed using an improved CFD-FE method. Comput Methods Biomech Biomed Eng 2025;28(3):314–25.
[11] Freitas SR, Andrade RJ, Larcoupaille L, Mil-Homens P, Nordez A. Muscle and joint responses during and after static stretching performed at different intensities. Eur J Appl Physiol 2015;115:1263–72.
[12] Fung Y-C, Fung Y-C. The meaning of the constitutive equation. In: Biomechanics: mechanical properties of living tissues; 1993. p. 23–65.
[13] Gao F, Grant TH, Roth EJ, Zhang L-Q. Changes in passive mechanical properties of the gastrocnemius muscle at the muscle fascicle and joint levels in stroke survivors. Arch Phys Med Rehabil 2009;90(5):819–26.
[14] Gracies J. Pathophysiology of spastic paresis. II: emergence of muscle overactivity. Muscle Nerve 2005;31(5):552–71.
[15] Granzier H, Labeit S. Structure–function relations of the giant elastic protein titin in striated and smooth muscle cells. Muscle Nerve 2007;36(6):740–55.
[16] Grasa J, Ramírez A, Osta R, Muñoz MJ, Soteras F, Calvo B. A 3D active-passive numerical skeletal muscle model incorporating initial tissue strains. Validation with experimental results on rat tibialis anterior muscle. Biomech Model Mechanobiol 2011;10(5):779–87. https://doi.org/10.1007/s10237-010-0273-z.
[17] Herzog W. The multiple roles of titin in muscle contraction and force production. Biophys Rev 2018;10:1187–99.
[18] Jakubowski KL, Terman A, Santana RVC, Lee SSM. Passive material properties of stroke-impaired plantarflexor and dorsiflexor muscles. Clin Biomech 2017;49:48–55. https://doi.org/10.1016/j.clinbiomech.2017.08.009.
[19] Jalal N, Gracies J-M, Zidi M. Mechanical and microstructural changes of skeletal muscle following immobilization and/or stroke. Biomech Model Mechanobiol 2020;19(1):61–80.
[20] Lee SSM, Spear S, Rymer WZ. Quantifying changes in material properties of stroke-impaired muscle. Clin Biomech 2015;30(3):269–75.
[21] Leng Y, Wang Z, Bian R, Lo WLA, Xie X, Wang R, et al. Alterations of elastic property of spastic muscle with its joint resistance evaluated from shear wave elastography and biomechanical model. Front Neurol 2019;10:736.
[22] Lu YT, Zhu HX, Richmond S, Middleton J. Modelling skeletal muscle fibre orientation arrangement. Comput Methods Biomech Biomed Eng 2011;14(12):1079–88. https://doi.org/10.1080/10255842.2010.509100.
[23] Millard M, Uchida T, Seth A, Delp SL. Flexing computational muscle: modeling and simulation of musculotendon dynamics. J Biomech Eng 2013;135(2):021005.
[24] Roots J, Trajano GS, Fontanarosa D. Ultrasound elastography in the assessment of post-stroke muscle stiffness: a systematic review. Insights Imaging 2022;13(1):67.
[25] Rutkowski NA, Sabri E, Yang C. Post-stroke fatigue: a factor associated with inability to return to work in patients <60 years—a 1-year follow-up. PLoS ONE 2021;16(8 August). https://doi.org/10.1371/journal.pone.0255538.
[26] Ryan AS, Dobrovolny CL, Smith GV, Silver KH, Macko RF. Hemiparetic muscle atrophy and increased intramuscular fat in stroke patients. Arch Phys Med Rehabil 2002;83(12):1703–7.
[27] Saadat F, Son J, Rymer WZ, Lee SSM. Frequency dependence of shear wave velocity in stroke-affected muscles during isometric contraction-preliminary data. In: 2018 40th annual international conference of the IEEE engineering in medicine and biology society (EMBC); 2018. p. 2292–5.
[28] Simon C, Rekik S, Zidi M. Effect of skeletal muscle immobilization on regional anisotropic viscohyperelastic properties change in a rat model. IRBM 2025;46(1):100868.
[29] Wheatley B. Anisotropic and viscoelastic tensile mechanical properties of aponeurosis: experimentation, modeling, and tissue microstructure; 2020.
[30] Xu W, Zheng Y, Jiang Y, Zhang Z, Ma S, Cao Y. Shear wave imaging the active constitutive parameters of living muscles. Acta Biomater 2023;166:400–8. https://doi.org/10.1016/j.actbio.2023.05.035.
[31] Zaleska-Dorobisz U, Kaczorowski K, Pawluś A, Puchalska A, Inglot M. Ultrasound elastography–review of techniques and its clinical applications. Brain 2013;6:10–4.
[32] Zhao H, Ren Y, Roth EJ, Harvey RL, Zhang L-Q. Concurrent deficits of soleus and gastrocnemius muscle fascicles and Achilles tendon post stroke. J Appl Physiol 2015;118(7):863–71.
[33] Zöllner AM, Pok JM, McWalter EJ, Gold GE, Kuhl E. On high heels and short muscles: a multiscale model for sarcomere loss in the gastrocnemius muscle. J Theor Biol 2015;365:301–10. https://doi.org/10.1016/j.jtbi.2014.10.036.